ELSEVIER

Materials Science and Engineering B59 (1999) 117–121

MATERIALS SCIENCE & ENGINEERING B

Epitaxial lateral overgrowth of GaN structures: spatially resolved characterization by cathodoluminescence microscopy and micro-Raman spectroscopy

F. Bertram [a,*], T. Riemann [a], J. Christen [a], A. Kaschner [b], A. Hoffmann [b], K. Hiramatsu [c], T. Shibata [d], N. Sawaki [d]

[a] *Institut für Experimentelle Physik, Otto-von-Guericke Universität, PO Box 4120, 39016 Magdeburg, Germany*
[b] *Institut für Festkörperphysik, Technische Universität Berlin, Hardenbergstraße 36, 10623 Berlin, Germany*
[c] *Department of Electrical and Electronic Engineering, Mie University, Mie 514-8507, Japan*
[d] *Department of Electronics, Nagoya University, Nagoya 464-01, Japan*

Abstract

The epitaxial lateral overgrowth of GaN structures is comprehensively characterized by scanning cathodoluminescence microscopy and micro-Raman spectroscopy. The samples under study consist of a 3-μm thick GaN buffer layer grown by MOVPE on (0001) sapphire and subsequently structured using a SiO_2 mask. The resulting stripe pattern is overgrown with HVPE GaN. Mask orientations along $\langle 1\underline{1}00\rangle$ and $\langle 11\underline{2}0\rangle$ are compared. CL microscopy directly visualizes the significant differences between the overgrown areas on top of the SiO_2-mask and the coherently grown regions between the SiO_2-stripes. The overgrown GaN shows a blue shift and a strong broadening of the luminescence. In contrast, the local luminescence from the areas of coherent (0001)-growth is dominated by narrow excitonic emission. The CL results are correlated with micro-Raman spectroscopy yielding information on the local strain and free carrier concentration. © 1998 Elsevier Science S.A. All rights reserved.

Keywords: GaN; ELOG; Excitonic luminescence; Spatially resolved cathodoluminescence; μ-Raman

1. Introduction

Recently, blue- or ultraviolet-emitting lasers have been developed using GaN- and InGaN-based compound semiconductors [1,2]. These device structures have been mainly grown on sapphire. However, several problems remain in nitride hetero-epitaxy, such as the reduction of dislocation density and its effect on luminescence and carrier transport. The defect structure of GaN films has been widely studied by transmission electron microscopy (TEM), primarily for threading dislocations in GaN films on the sapphire substrate. The very promising approach of epitaxial lateral overgrowth (ELO) has already been proven effective in reducing dislocation density in GaAs- and InP-layers on Si substrates [3–5]. Recently, this process has been successfully applied to GaN [6–12]. However, there is still a lack of understanding of the microscopic mechanisms involved.

In this paper we present the first comprehensive microscopic characterization by cathodoluminescence microscopy and μ-Raman spectroscopy sensing and correlating the local optical and electronic properties of ELO GaN structures and their dependencies on the orientation of the pattern.

2. Experimental setup

The epitaxial lateral overgrowth (ELO) structures investigated here are schematically outlined in Fig. 1. A 3-μm thick GaN layer is grown by MOVPE on (0001) sapphire and patterned with stripes of a 120 nm thick SiO_2 mask. The parallel SiO_2 stripes are ordered in $\langle 11\underline{2}0\rangle$ direction for sample A (Fig. 1(a)) or in $\langle 1\underline{1}00\rangle$ direction for sample B (Fig. 1(b)), respectively, and the width of the windows and the masks are 10 μm each. The lateral overgrowth is achieved using 50 μm thick

* Corresponding author. Tel.: +49-391-6712144; fax: +49-391-6711130.
E-mail address: frank.bertram@physik.uni-magdeberg.de (F. Bertram)

PII: S0921-5107(98)00329-8

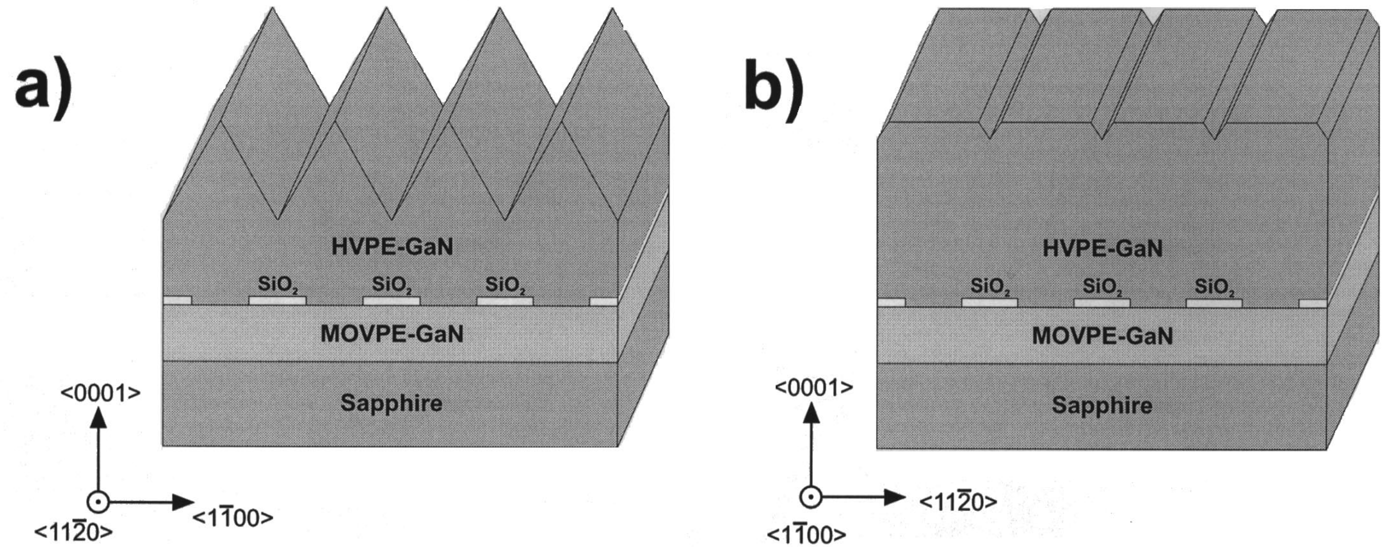

Fig. 1. Schematic structure of the ELOG sample with SiO_2 pattern along the $\langle 1120 \rangle$ (a) and along the $\langle 1100 \rangle$ (b) direction.

hydride vapor phase epitaxy (HVPE) GaN deposited on the underlying MOVPE GaN layer through the windows in the SiO_2 mask.

The low-temperature (5 K) cathodoluminescence (CL) measurements were performed in a fully computer-controlled modified scanning electron microscope (SEM). In the CL imaging mode the focused electron beam is scanned over the area of interest (256 × 200 pixels) and complete CL spectra are recorded at each pixel and stored. The resulting three-dimensional data set $I_{CL}(x, y, \lambda)$ is ex situ evaluated to produce local spectra, sets of monochromatic CL images as well as CL wavelength images (CLWI) mapping the emission wavelength of the local maximum CL intensity at each sampling point. A spatial resolution better than 40 nm can be achieved at suitable low acceleration voltage (typical 3 kV). Details and applications of this technique are described elsewhere [13].

Micro-Raman measurements were carried out in backscattering geometry using a triple-grating spectrometer equipped with a confocal micro optic and a cooled charge-coupled device (CCD) detector. The 515.4 nm line of an Ar^+-Kr^+ mixed-gas laser was used for excitation. With this setup we are able to detect line positions with an accuracy of 0.1 cm^{-1}. The spatial resolution of the Raman setup is better then 1 μm.

3. Results and discussion

Cross sectional CL mappings are presented in Fig. 2 for both samples. The scanning electron microscope (SEM) images of the resulting ELOG structures depicted in Fig. 2(a and d) demonstrate the strikingly different overgrowth schemes: While for the ⟨1120⟩-direction, sample A (Fig. 2(a)), the HVPE layer is terminated by sharply defined ⟨1101⟩-facets, an almost smooth lateral overgrowths results for the ⟨1100⟩-orientation, sample B (Fig. 2(d)). The strongly varying local CL emission wavelength is mapped in the CLWIs in Fig. 2(b and e), as well as in further magnified views in Fig. 2(c and f), respectively.

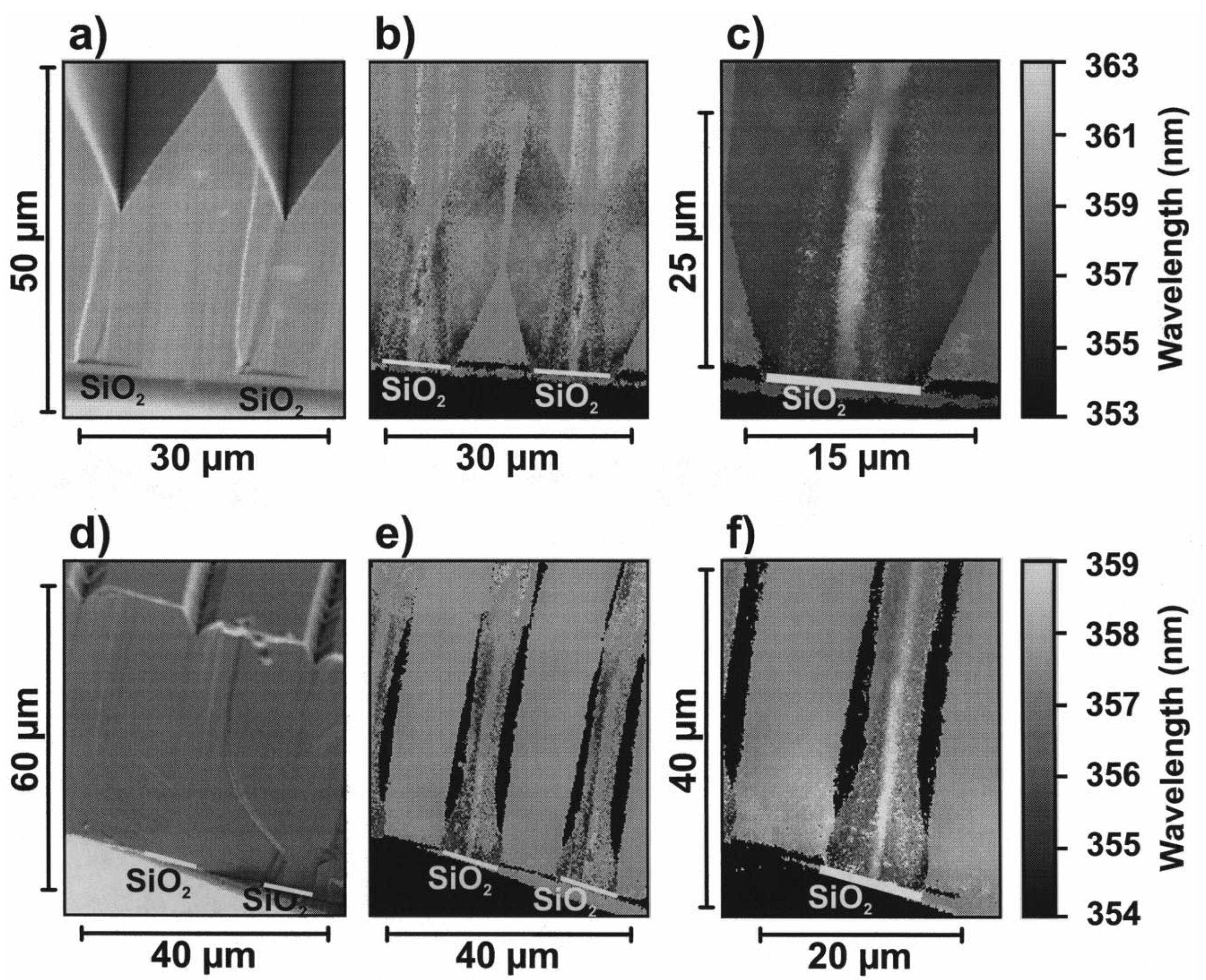

Fig. 2. SEM image, CLWI and magnified CLWI of both samples: ⟨1120⟩ orientation in the upper row and ⟨1100⟩ orientation in the bottom row.

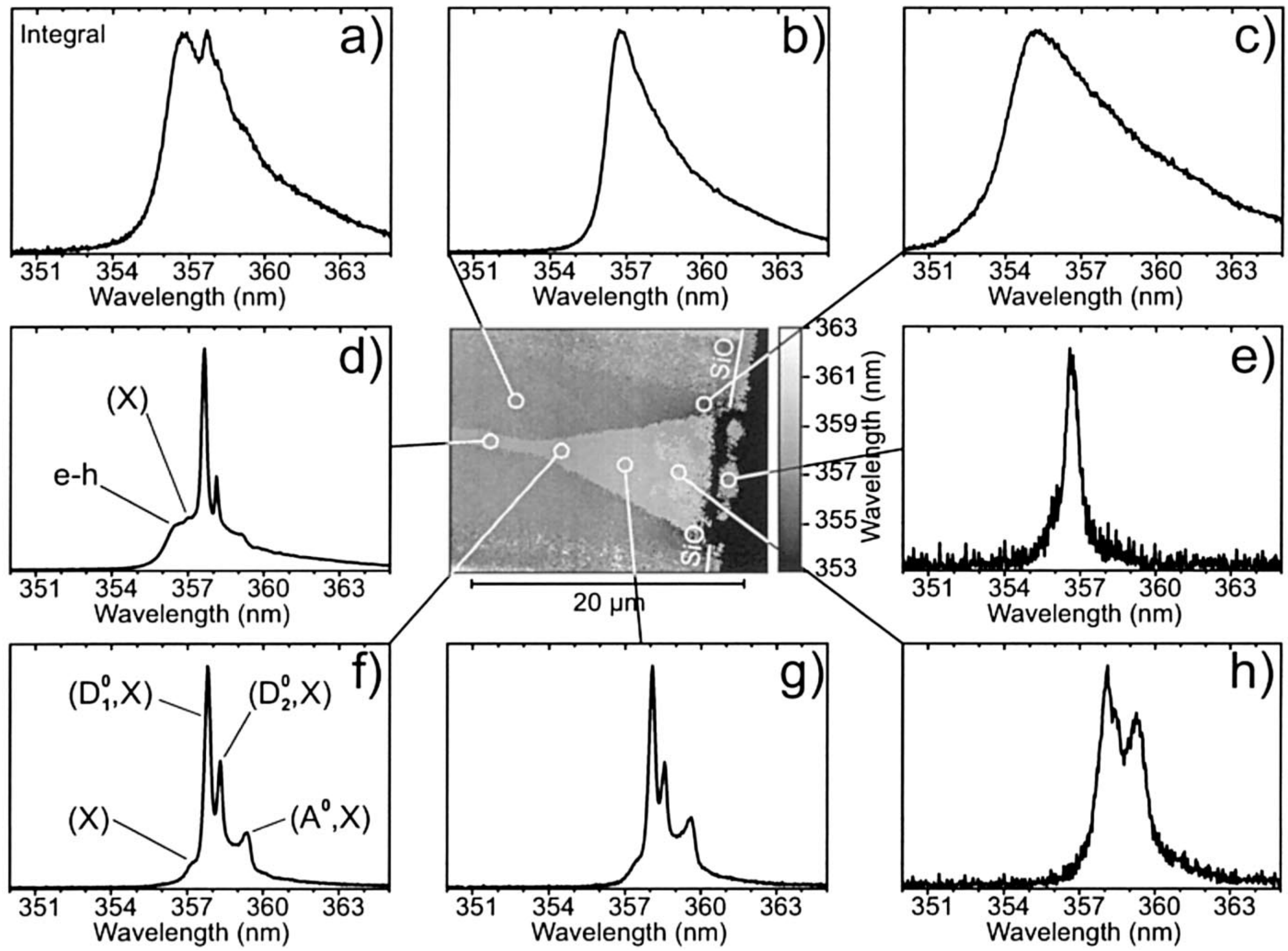

Fig. 3. Local spectra from the coherently grown region of the ELOG sample with SiO_2 stripes in ⟨1120⟩ direction.

The CLWI in Fig. 2(b) visualizes three different growth regions: the GaN buffer layer, the overgrown region above the SiO_2 and the area of coherent growth between the SiO_2 pattern. The buffer layer shows a blue-shifted (D^0, X) emission at 356.4 nm according to a compressive biaxial stress of 0.8 GPa [14]. In the coherent growth region a monochromatic triangle of almost homogeneous emission at 358 nm is visible evolving in the center between the SiO_2 stripes (Fig. 2(b)). The overgrowth region (CLWI with higher magnification in Fig. 2(c)) is dominated by a blue-shifted emission around 356 nm and is very inhomogeneous showing stripe-like patterns in c-direction. Strongly red shifted, extrinsic CL (362 nm) dominates the very center of the overgrowth region, i.e. the ELO coalescence area. At the outer edges of the SiO_2 stripes a strong blue-shift (354 nm) is obtained. Areas with no CL intensity are masked out in black in the CLWIs.

The lower row of Fig. 2(d–f) depicts the results for sample B (SiO_2-pattern along ⟨1100⟩). Again the three different growth regions can be separated. However, here the coherently grown region forms a uniform rectangle proceeding now up to the surface. The blue-shifted overgrowth region is even more inhomogeneous than for sample A. Again the coalescence area is marked by strongly red shifted, extrinsic luminescence in the center of the overgrowth region. A strongly blue shifted emission arises from the edges of the SiO_2 stripes due to local compressive strain.

Fig. 3 shows a set of local spectra from the coherently grown region of sample A. The different positions of these spectra are indicated in the central CLWI. Starting with the local CL from the buffer (Fig. 3(e)) various points aligned along a line orientated in ⟨0001⟩ direction crossing over the triangle of the coherently grown region are marked. Spectra from these points clearly show sharp excitonic CL-lines: (FX), (D_1^0, X), (D_2^0,X) and (A^0, X) are well resolved (assignment of the transitions in Fig. 3(f) according to Siegle et al. [15]). With increasing distance to the interface (i.e. scanning from Fig. 3(d–h)) a simultaneous blue shift of 8 meV is observed for all 4 lines and a high energy shoulder evolves (see Fig. 3(d)) due to electron hole plasma inter-band recombination. This process evidencing large local free carrier concentration leads to the broad and strongly blue-shifted CL emission outside the triangle (see Fig. 3(b and c)).

In order to understand the spatial dependence of the luminescence we performed μ-Raman scattering-experiments in the same region where the CL microscopy was carried out. By measuring the E_2 mode we detected the local strain distribution [16]. The free carrier concentration was determined by the position of the LPP modes [17]. Fig. 4 shows the results of different μ-Raman linescans over the cross section of sample A. The two different scans are marked by a gray and a black line, respectively, in the CLWI (inset of Fig. 4(a)) and in the SEM image (inset of Fig. 4(b)). The free carrier concentration in the overgrown region jumps to a value of about 9×10^{18} cm^{-3} outside the buffer layer and remains nearly constant up to the surface. This results from a strong impurity incorporation in the overgrown area. The free carrier concentration in the coherently grown region starts at a level below our detection limit of about 1.0×10^{18} cm^{-3}. At a distance of 14 μm from the substrate interface a jump occurs to a high value of 1.3×10^{19} cm^{-3}. In comparison with the CLWI we obtain this increase of the carrier concentration at the end of the coherently grown region (at the top of the triangle, compare Fig. 2(b)). In the coherently grown region we find a lower carrier concentration due to less structural defects. In Fig. 4(b) the biaxial stress determined by the shift of the E_2 mode is depicted. The compressive stress in the coherently grown region decreases continuously from a value of 0.5 GPa in the buffer layer with increasing distance from the substrate and is fully relaxed at the surface. The compressive stress in the overgrown region on the top of SiO_2 relaxes much faster than in the coherently grown region. At 10 μm from the interface the stress reduction stops. At the surface we find a compressive stress of 0.2 GPa, which fits the value at the same distance from the substrate in the coherently grown region.

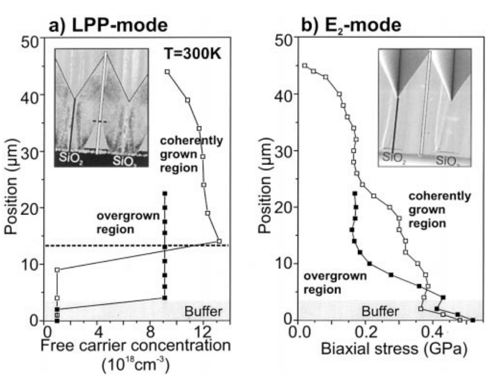

Fig. 4. μ-Raman linescans: gray line (coherently grown region) and black line (overgrown region); (a) Free carrier concentration determined from the LPP-mode and (b) biaxial (compressive) stress calculated from the E_2-Raman-mode.

4. Conclusion

Epitaxial lateral overgrowth GaN structures with SiO_2 mask orientated along ⟨1120⟩ and ⟨1100⟩ were characterized and regions of different growth regimes were identified. In both ELO structures the coherently grown region shows perfect excitonic CL, i.e. crystallographic quality. In the ELO sample with SiO_2 stripes in ⟨1120⟩ direction the coherently grown area forms a sharply defined triangle in the middle of the structure. This pattern orientation shows a strong ⟨1$\underline{1}$00⟩ facetting in the surfaces morphology. In the sample with pattern along ⟨1100⟩ the coherently grown region forms a rectangle of sharp excitonic luminescence up to the surface indicating perfect crystallographic quality and low carrier concentration in perfect agreement with further μ-Raman results [18]. The overgrown region is dominated by a blue shifted broad CL emission with a strong red shifted line in the coalescence area. This is due to a strong impurity incorporation at the merging crystal planes and resulting voids. At the edges of the SiO_2 stripes blue shifted broad luminescence indicates a high dislocation density and a strong impurity incorporation as found in TEM images.

References

[1] S. Nakamura, M. Senoh, S. Nagahama, et al., Jpn. Appl. Phys. 35 (1996) 74.
[2] I. Akasaki, S. Sota, H. Sakai, T. Tanaka, M. Koike, H. Amano, Electron Lett. 32 (1996) 1105.
[3] D. Pribat, B. Gerad, M. Dupuy, P. Legagneux, Appl. Phys. Lett. 60 (1992) 2144.
[4] S.F. Fang, K. Adomi, S. Iyer, H. Morkoc, H. Zabel, C. Choi, N. Otsuka, Appl. Phys. Lett. 68 (1992).
[5] S.D. Lester, F.A. Ponce, M.G. Craford, D.A. Steigerwald, Appl. Phys. Lett. 66 (1996) 1249.
[6] A. Sakai, Appl. Phys. Lett. 71 (1997) 2259.
[7] D. Kapolnek, S. Keller, R. Ventury, R.D. Underwood, P. Kozodoy, S.P. Den Baars, U.K. Mishra, Appl. Phys. Lett. 71 (1997) 1204.
[8] A. Usui, H. Sunakawa, A. Sakai, A.A. Yamaguchi, Jpn. J. Appl. Phys. 36 (1997) 899.
[9] T.S. Zheleva, O.H. Nam, M.D. Bremser, R.F. Davis, Appl. Phys. Lett. 71 (1997) 2472.
[10] D. Kapolnek, X.H. Wu, B. Heying, S. Keller, B.P. Keller, U.K. Mishra, S.P. DenBaars, J.S. Speck, Appl. Phys. Lett. 67 (1995) 1541.
[11] S. Nakamura, M. Senoh, S. Nagahama, et al., Appl. Phys. Lett. 72 (1998) 211.
[12] O.-H. Nam, M.D. Bremser, T. S. Zheleva, R.F. Davis, Appl. Phys. Lett. 71 (1997) 2638.
[13] J. Christen, M. Grundmann, D. Bimberg, J. Vac. Sci. Technol. B9 (1991) 2358.
[14] C. Kisielowski, J. Krüger, S. Ruvimov, et al., Phys. Rev. 54 (1996) 17745.
[15] H. Siegle, A. Hoffmann, L. Eckey, et al., Appl. Phys. Lett. 71 (1997) 2490.
[16] C. Kisielowski, J. Krüger, S. Ruvimov, et al., Phys. Rev. 55 (1997) 4907.
[17] P. Perlin, J. Camassel, W. Knap, et al., Appl. Phys. Lett. 67 (1995) 2524.
[18] F. Bertram, T. Riemann, J. Christen, A. Kaschner, A. Hoffmann, K. Hiramatsu, Appl. Phys. Lett. submitted.